The Effects of Gamma Irradiation on Molecular Weight, Morphology and Physical Properties of PHBV/Cloisite 30B Bionanocomposites

Kahina Iggui, Mustapha Kaci, Mohamed Mahlous, Nicolas Le Moigne, Anne Bergeret

Journal of Renewable Materials

Tech Science Press

The Effects of Gamma Irradiation on Molecular Weight, Morphology and Physical Properties of PHBV/Cloisite 30B Bionanocomposites

Kahina Iggui[1,2,*], Mustapha Kaci[1], Mohamed Mahlous[3], Nicolas Le Moigne[4] and Anne Bergeret[4]

[1]Laboratoire des Matériaux Polymères Avancés (LMPA), Université de Bejaia, 06000 Bejaia, Algeria.

[2]Institut de Technologie, Université Akli Mohand Oulhadj, Bouira 10000, Algeria.

[3]Centre de Recherche Nucléaire d'Alger (CRNA), Boulevard Frantz Fanon, Alger 16000, Algeria.

[4]Centre des Matériaux des Mines d'Alès (C2MA)[a], IMT Mines Alès, Université de Montpellier, 6 avenue de Clavières, 30319 Alès Cedex, France.

[3] C2MA is member of the European Polysaccharide Network of Excellence (EPNOE), http://www.epnoe.eu.

[*]Corresponding Author: Kahina Iggui. Email: iguikahina@yahoo.fr.

Abstract: In this paper, the effects of gamma irradiation on Cast poly(3-hydroxybutyrate-co-3-hydroxyvalerate) (PHBV) and PHBV/Cloisite 30B (C30B) (3 wt%) bionanocomposite prepared by melt compounding, were evaluated at various doses, i.e., 5, 15, 20, 50 and 100 kGy at room temperature in air. Changes in molecular weight, morphology and physical properties were investigated. The study showed that the main degradation mechanism occurring in gamma irradiation in both Cast PHBV and C-PHBV/3C30B bionanocomposite is chain scission, responsible for the decrease of molecular weight. Differential scanning calorimetry (DSC) data indicated a regular decrease in crystallization temperature, melting temperature and crystallinity index for all irradiated samples with increasing the dose. Further, DSC thermograms of both Cast PHBV and PHBV bionanocomposite exhibited double melting peaks due probably to changes in the PHBV crystal structure. Tensile and DMA data showed a reduction in Young's modulus, strength, elongation at break and storage modulus with the radiation dose; the decrease was however more pronounced for Cast PHBV. The morphological damages were much less pronounced for the PHBV bionanocomposite sample compared to Cast PHBV, for which some irregularities and defects were observed at 100 kGy. This study highlighted the ability of C30B to counterbalance the detrimental effect of radiolytic degradation on the functional properties of PHBV up to 100 kGy, thus acting as a potential anti-rad.

Keywords: Poly(3-hydroxybutyrate-co-3-hydroxyvalerate) (PHBV); bionano-composite; cloisite 30B; gamma irradiation; degradation

1 Introduction

Today, biopolymers such as polyhydroxyalcanoates and their bionanocomposites are currently used in short-term applications such as food packaging and biomedical due to their biodegradability and biocompatibility [1]. However in such applications, biodegradable polymers have to be sterilized by ionizing radiations including gamma rays, e-beam, etc. before utilization in order to minimize any risk of bacterial contamination [2]. On the other hand, the ionizing radiation process if not controlled, may result in the polymer degradation through chain scission mechanism and/or cross-linking affecting the final material properties [3,4]. Indeed, in the family of polyhydroxyalcanoates, many studies have been carried out on the effects of gamma irradiation on the properties of poly(3-hydroxybuterate) (PHB3) and

poly(3-hydroxybuterate-co-3-hydroxyvalerate) (PHBV). In this regard, Luo et al. [5] investigated the effects of gamma irradiation at 100 and 250 kGy on the molecular weight and mechanical and thermal properties of PHBV in air. The results indicated a decrease in the molecular weight due to chain scission. A reduction in both thermal and tensile properties was also observed, while Young's modulus remained almost unchanged. Mitomo et al. [6] reported the gamma irradiation effects on thermal properties and biodegradation of PHB and PHBV. It was found a decrease in both the glass transition and melting temperatures attributed to the chain scission mechanism, which took place within amorphous regions below 100 kGy and in the crystalline regions at higher doses. Furthermore, the biodegradation rate of PHB and PHBV was also accelerated under gamma irradiation. The effects of gamma irradiation on the molecular weight, thermal properties and crystallinity of PHB and PHBV were investigated by Oliveira et al. [7]. The authors reported a decrease in the molecular weight as a result of chain scission mechanism and an increase in the degree of crystallinity due to chemi-crystallization process. Hermida et al. [8] investigated the effects of gamma irradiation on the mechanical properties of PHB and PHBV. It was reported that both materials exhibited similar behavior characterized by a decrease in the tensile strength and elongation at break, while the tensile modulus remained almost constant with increasing radiation doses. Furthermore, the authors correlated well the decrease in molecular weight with elongation at break. A linear relationship between the two characteristics was established. Recently, gamma irradiation effects on functional properties of nanocomposites materials have been the object of many publications. Zaidi et al. [9] investigated the effect of gamma irradiation on the chemical structure and properties of PLA and PLA/C30B nanocomposites in air up 200 kGy. FTIR data indicated that the transformation of ester groups of PLA under gamma irradiation led to the formation of various oxidative species such as hydroperoxides, alcohols, carboxylic acids and diketone end groups. Similar chemical changes were also observed in the presence of C30B and no shift of the absorption band position was observed. The authors stated that both irradiated PLA and PLA/30B have undergone the same degradation mechanism. The only difference was the degradation rate, which was higher in the neat PLA compared to PLA/30B nanocomposite. This behavior was explained as a result of a better dispersion of C30B in PLA matrix and a relative ordered structure of C30B nanoclay formed after gamma irradiation exposure. Further, Zembouai et al. [10] reported that carbonyl groups were the main oxidative products formed in PHBV/PLA blends upon gamma irradiation even in the presence of PHBV-*g*-MA compatibilizer and organo-modified montmorillonite. A decrease in the molecular weight was measured and attributed to chain scission mechanism. However, the degradation was more pronounced for the unfilled and uncompatibilized PHBV/PLA blends. In another paper, Zembouai et al. [11] investigated the effect of e-beam irradiation on the properties and ecotoxicity of PHBV/PLA blends in presence of C30B up to 10 kGy. The authors reported that eventhough, e-beam irradiation induced a decrease in the functional properties of the materials, there is however, no toxic species detected in the irradiated samples. Marra et al. [12] investigated the effect of ZnO and gamma irradiation treatment on PLA and PLA/5% ZnO films, singularly and combined, on the shelf life of packed ham inoculated with bacteria suspension of L. innocua, E. coli and S. enterica. The samples were irradiated with a γ-radiation dose of 0.3 kGy at dose rate of 13.5 kGy/h. Microbiological analysis was performed at 0, 1 and 5 days on samples stored at 4 °C. The authors reported that the only presence of ZnO on PLA surface film, wrapping the ham, was not sufficient to reduce significantly the bacteria. The combined treatments, instead, induced a higher reduction of bacteria, showing a complete inhibition of S. enterica and E. coli after 5 days of storage. Mizera et al. [13] investigated the effects of beta radiation on mechanical properties of polyamide 11 (PA11) at 23°C and 80°C with a dose range between 0 and 198 kGy. The results showed that the beta irradiation slightly improves the PA11 tensile strength and E-modulus at ambient temperature. However at 80°C, the tensile behaviour of PA11 is worse than at 23°C. Aouat et al. [14], investigated the effects of gamma irradiation on both morphology and properties of neat poly(lactic acid) (PLA), PLA/microcrystalline cellulose (MCC) and PLA/cellulose nanowhiskers (CNW), prepared by melt spinning in presence of (PLA-*g*-MA) used as the compatibilizer up to 30 kGy. The results indicated that up to 20 kGy, the property changes of the irradiated fibers were negligible. However, at 30 kGy, the thermal and tensile properties were significantly decreased. However, the incorporation of cellulosic

fillers in PLA fibers, in particular MCC, was found to hinder the radiolytic degradation process of the irradiated samples. The effects of three different sterilization techniques, Electron beam (β-irradiation), gamma and X-ray irradiation with two different doses (25 and 33 kGy) on properties of poly-(ε-caprolactone) fiber mats were reported by Cassan et al. [15]. It was found that properties of irradiated samples were affected by all three sterilization techniques. The irradiation led to a polymer chain scission and a decreased molecular weight. The effect was more pronounced for higher irradiation doses. Crystallinity of fiber mats increased significantly, while melting temperature and glass transition temperature were almost unchanged. However, the mechanical properties did not change significantly upon irradiation. From the above studies, it appears clearly that further studies are necessary on PHBV/C30B bionanocomposites to better understanding their withstanding against gamma irradiation. Moreover to the best of our knowledge, no published data are available yet on the behavior of PHBV/ Cloisite 30B© bionanocomposites under ionizing radiation. Therefore, the goal of this work was to investigate the effects of gamma irradiation on the molecular weight, morphology and thermal, mechanical and thermo-mechanical properties of PHBV/Cloisite 30B (3 wt%) bionanocomposite with respect to neat PHBV. The materials were exposed to gamma irradiation at room temperature in air at increasing doses, i.e., 5, 15, 25, 50 and 100 kGy. The changes in molecular weight, morphology and physical properties of the irradiated samples were evaluated by several techniques, including size exclusion chromatography (SEC), differential scanning calorimetry (DSC), thermogravimetric analysis (TGA), dynamic mechanical analysis (DMA), tensile testing, scanning electron microscopy (SEM) and transmission electron microscopy (TEM).

2 Experimental

2.1 Materials and Preparation of PHBV/Cloisite 30B Bionanocomposite

Poly (3-hydroxybutyrate-co-3-hydroxyvalerate) (PHBV) named PHI 002® and Cloisite 30B were supplied by NaturePlast (France) and Southern Clay Products, Inc. (USA) respectively.

The PHBV and bionanocomposite sheet samples, named Cast PHBV and C-PHBV/3C30B (prepared at a C30B content of 3 wt%) respectively were produced by masterbatch dilution with neat PHBV using a single-screw cast extruder. Our previous study [16] detailed the method of preparation of masterbatch and bionanocomposite sheet, and demonstrated the formation of intercalated bionanocomposites.

2.2 Gamma Irradiation Test

The sheet samples in rectangular form (5 × 5 cm) of both Cast PHBV and C-PHBV/3C30B (3 wt%) bionanocomposite were subjected to gamma irradiation at room temperature in air using Co^{60} industrial equipment at the Nuclear Research Center of Algiers (CRNA). The samples were subjected to various doses, i.e., 5, 15, 20, 25, 50 and 100 kGy, at a dose rate of 1.92 Gyh^{-1}.

2.3 Characterization Methods

2.3.1 Solubility Test

To verify if any gel fraction was formed in Cast PHBV and C-PHBV/3C30B bionanocomposite samples during gamma irradiation exposure, solubility test was performed. Approximately 1 g of dry irradiated and non-irradiated Cast PHBV and C-PHBV/3C30B bionanocomposite samples were placed in a Soxhlet apparatus and extracted with 100 ml of chloroform at 60°C for 1 h [17].

2.3.2 Size-Exclusion Chromatography (SEC)

The molecular weight changes of Cast PHBV and C-PHBV/3C30B bionanocomposites samples before and after gamma irradiation were determined by size-exclusion chromatography (SEC) using an Omni-SECT 60A system. Cast PHBV and C-PHBV/C30B bionanocomposites (typically 20 mg) were dissolved in 2 ml of chloroform over 1 h at 60 C. Before injection, all samples were filtered through a Phenex PTFE 0.2 mm filter to remove any insoluble fractions or clay. SEC experiments were conducted

in a Waters 410 differential refractometer using a PL Gel 5-mm Mixed-C column (1 × 600 mm). The column eluent was chloroform at a flow rate of 1 mL/min and polystyrene standards were used for calibration. The weight and number averages molecular weights $\overline{M_w}$ and $\overline{M_n}$ as well as the polydispersity index Đ were determined. Two specimens of each sample were tested, and the average results were reported.

2.3.3 Differential Scanning Calorimetry (DSC)

Differential scanning calorimetry analysis was performed on a Pyris Diamond DSC thermal analysis system (PerkinElmer) equipped with an Intra Cooler II. Heating and cooling scans were performed at a scanning rate of 10°C min^{-1} from 30 to 200°C, using N_2 as the purging gas. Small amounts (15-20 mg) of dried samples were placed into aluminum pans. At least three specimens were tested for each sample. The degree of crystallinity (X_c) was determined according to Eq. (1):

$$X_c = \frac{\Delta H_m}{W.\Delta H_m^0} \times 100 \quad (1)$$

where ΔH_m ($J.g^{-1}$) is the melting enthalpy of the polymer matrix PHBV, W is polymer weight fraction (PHBV) in the sample, calculated from the real content of C30B, and ΔH_m^0 is the melting enthalpy of a pure crystal and ΔH_m^0 = 146 $J.g^{-1}$ found for PHB by Barham et al. [18]. No values for PHBV with varying valerate amounts are referenced in literature.

2.3.4 Thermo Gravimetric Analysis (TGA)

Thermogravimetric analysis measurements were carried out using a Pyris Diamond thermogravimetric analyzer (PerkinElmer) on specimens of 10-12 mg, under nitrogen atmosphere, at a heating rate of 10 °C/min. Samples were heated from room temperature up to 700°C. Three specimens were tested for each sample.

2.3.5 Dynamic Mechanical Analysis (DMA)

The thermo-mechanical behavior of Cast PHBV and C-PHBV/3C30B bionanocomposite samples was investigated in the vicinity of the α-transition using a DMA 50 dynamic mechanical analyzer (Metravib O3dB, France). Three rectangular specimens of each sample with a dimension of approximately 35 × 5 × 0.5 mm were tested. The measurements were performed in shear mode at 5 Hz and 5 µm of amplitude and the temperature was varied from -20 to 120°C at a heating rate of 3 °C/min. Storage modulus (G'), loss modulus (G") and loss factor (tan δ) were determined.

2.3.6 Tensile Testing

The mechanical properties were measured with a universal testing machine (MTS) at room temperature according to ASTM standard method (ISO 527). The tensile strength and tensile modulus were recorded from the stress-strain curves for the different tensile test pieces. The extension was set at 1 mm/min. Five specimens of each sample were tested and mechanical tensile data were calculated from an average of five specimens for each sample.

2.3.7 Scanning and Transmission Electron Microscopy (SEM and TEM) Observations

Fractured surfaces of Cast PHBV and C-PHBV/3C30B bionanocomposite films were observed using a Quanta 200 FEG (FEI Company) environmental scanning electron microscope at an acceleration voltage of 7 to 10 keV. Prior to observations in scanning mode (SEM), the fracture surfaces of the films were sputter coated with carbon using a Carbon Evaporator Device CED030 (Balzers), to ensure good surface conductivity and avoid any degradation. For STEM observations, the different samples were

prepared using an ultramicrotome (Leica Ultracut) equipped with a diamond knife. The ultrathin sections were cut at -80°C and were deposited on Cu grids.

3 Results and Discussion

3.1 Solubility Test

The solubility test of both neat PHBV and PHBV/C30B bionanocomposite in the chloroform at 60°C showed that before gamma irradiation, neat PHBV, Cast PHBV and C-PHBV/3C30B samples were totally soluble in the solvent. After gamma irradiation exposure, it was also found that no cross-linked fraction was obtained whatever the sample and the dose, which support that no cross-linking reaction occurred between PHBV chains and/or organo-modifier of C30B.

3.2 Molecular Weight Changes

Tab. 1 reports the values of the weight average molecular weight $\overline{M_w}$, number average molecular weight $\overline{M_n}$ and polydispersity index (Đ) for Cast PHBV and C-PHBV/3C30B bionanocomposite before gamma irradiation exposure and at 50 and 100 kGy. From Tab. 1, it is noted a significant reduction in $\overline{M_w}$ and $\overline{M_n}$ for both Cast PHBV and C-PHBV/3C30B bionanocomposite. Indeed, at 100 kGy, Cast PHBV exhibit a decrease in $\overline{M_w}$ and $\overline{M_n}$ by almost 77 and 74% compared to that of non-irradiated sample, respectively. Similar trend is also observed for $\overline{M_w}$ and $\overline{M_n}$ of C-PHBV/3C30B bionanocomposite, whose values decrease by about 78 and 71% at 100 kGy, respectively.

Table 1: Weight-average molecular weight ($\overline{M_w}$), number average molecular weight ($\overline{M_n}$) and polydispersity index (Đ) of Cast PHBV and C-PHBV/3C30B bionanocomposite as function of irradiation dose

Samples	Dose (kGy)	$\overline{M_w}(g/mol)$	$\overline{M_n}(g/mol)$	Đ
Cast PHBV	0	290862 ± 2881	112957 ± 12632	2.6 ± 0.26
	50	99489 ± 3259	43545 ± 1677	2.3 ± 0.01
	100	65758 ± 819	28954 ± 88	2.3 ± 0.03
C-PHBV/3C30B	0	305510 ± 1971	94648 ± 5460	3.2 ± 0.17
	50	100717 ± 1126	42541 ± 211	2.3 ± 0.05
	100	66053 ± 753	27435 ± 214	2.4 ± 0.05

The decrease in both $\overline{M_w}$ and $\overline{M_n}$ may result from the oxidative degradation of the irradiated samples. Further, the value of polydispersity index close to 2 suggests that chain scission mechanism is prevalent in cast PHBV and C-PHBV/3C30B, which likely occurs randomly in the amorphous regions of the polymer materials [19,20]. It is also worthy to indicate that no cross-linking fraction is formed during gamma irradiation exposure of the samples as revealed by the solubility test.

3.3 Changes in the Crystalline Structure

The DSC results on crystallization (T_c), melting (T_m) temperatures and crystallinity index (X_c) determined from cooling and second heating scans for Cast PHBV and C-PHBV/3C30B bionanocomposite as a function of irradiation doses are reported in Tab. 2. Fig. 1 shows the second heating curves of Cast PHBV and C-PHBV/3C30B as a function of irradiation dose from 5 to 100 kGy.

Table 2: Thermal characteristics (crystallization temperature Tc, melting temperature Tm and crystalline index Xc) obtained from the cooling and the second heating of Cast PHBV and C-PHBV/3C30B bionanocomposite as function of irradiation dose

Samples	Dose (kGy)	T_c (°C)	T_{m2}(°C)	T_{m1} (°C)	X_c (%)
PHBV	0	119 ± 0.2	-	170 ± 0.5	66.1 ± 1
	5	118 ± 0.4	-	168 ± 0.5	67.0 ± 0.5
	15	117 ± 0.1	-	166 ± 0.5	65.8 ± 1
	25	114 ± 0.3	-	165 ± 1	63.6 ± 0.5
	50	115 ± 0.2	163 ± 0.3	167 ± 1	63.5 ± 1
	100	113 ± 0.3	157 ± 0.1	164 ± 0.5	60.2 ± 1
PHBV/3C30B	0	119 ± 0.1	-	165 ± 0.5	63.3 ± 0.5
	5	119 ± 0.3	-	165 ± 1	65.2 ± 0.5
	15	118 ± 0.3	162 ± 1	167 ± 1	64.3 ± 1
	25	117 ± 0.1	161 ± 0.1	166 ± 0.5	63.5 ± 1
	50	116 ± 0.5	159 ± 0.5	164 ± 0.5	61.5 ± 1
	100	113 ± 0.1	155 ± 0.6	162 ± 0.5	58.8 ± 1

For all samples, a decrease of the melting (T_m) temperature is observed with increasing the irradiation doses. Thermograms of samples irradiated above 15 kGy exhibits double melting peaks composed of a shoulder related to the main peak (T_{m1}) observed for non-irradiated and low irradiated samples and a second peak (T_{m2}) appearing at a lower temperature. According to the literature [7,8,20], the formation of a secondary melting peak at low temperature is attributed to degradation through chain scission mechanism and the ability of the short chains to reorganize themselves. In addition, the occurrence of different crystal populations with different lamellar thickness could also be responsible for the formation of a secondary melting peak. The decrease in T_m with irradiation dose is thus attributed to the melting of crystals of lower thermal stability composed of lower molecular weight polymer chains [21-23].

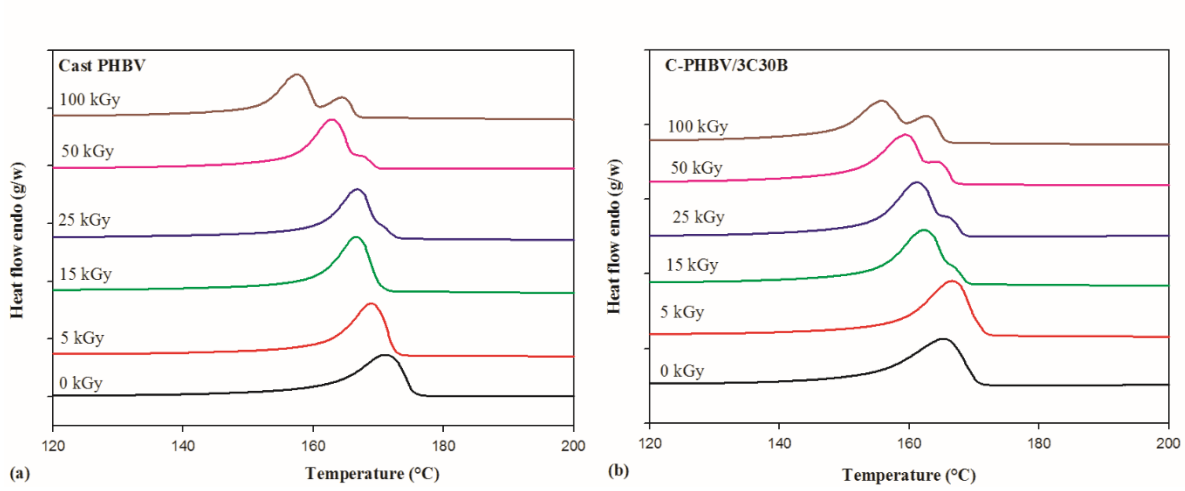

Figure 1: DSC thermograms of (a) Cast PHBV and (b) C-PHBV/3C30B bionanocomposite during second heating scans at various doses

Figs. 2(a), 2(b) show the relationship between crystallization temperature (T_c), crystalline index (X_c) and irradiation dose for Cast PHBV and C-PHBV/3C30B. A roughly linear relationship is observed, the T_c and X_c decrease as the dose increases. The decrease of T_c is attributed to scission chain, which promotes the formation of shorter molecules with higher mobility that can rearrange into new crystalline structure at lower temperature [24,25]. While the decrease of X_c could be due to the destruction of crystallites by gamma irradiation resulting in imperfections in the crystalline structure [26].

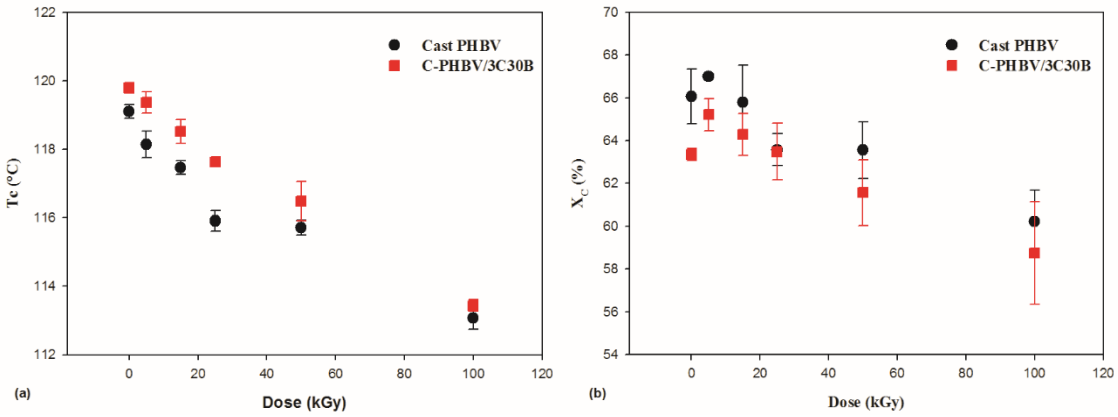

Figure 2: Evolution of (a) crystallization temperature Tc, (b) crystalline index Xc of Cast PHBV and C-PHBV/3C30B bionanocomposite as function of dose

3.4 Thermal Stability Changes

Changes in thermal stability induced by gamma irradiation exposure of Cast PHBV and C-PHBV/3C30B bionanocomposite were investigated by TGA. The values of thermal characteristics as main degradation temperature at 5%, 50% weight loss, the maximum degradation rate, and the char percentage are summarized in Tab. 3. According to the data reported in Tab. 3, the C-PHBV/3C30B bionanocomposite exhibits a higher thermal stability compared to the Cast PHBV before exposure to gamma irradiation. This is due to the presence of organoclay C30B which reduce the diffusion of the volatile degradation products of the bionanocomposite sample [27,28]. After exposure to gamma irradiation, a decrease in the degradation temperatures with increasing irradiation dose is observed for both materials. For Cast PHBV, the temperature degradation $T_{5\%} = 263°C \pm 1$ is decreases by 5°C at 100 kGy. For the bionanocomposite sample, $T_{5\%}$ shifts also to a lower value passing from 266°C ± 1 to 259 ± 0.5. The reduction in thermal stability is due to the reduction of the molecular weight of the irradiated samples that arise as radiolysis products. There are thus no significant differences of thermal stability between cast PHBV and the bionanocomposite and its evolution after gamma irradiation is similar for both materials. Accordingly, it can be concluded that the presence of C30B have no positive influence on maintaining thermal stability of PHBV after gamma irradiation.

Table 3: The decomposition temperatures at 5%, 50% weight loss, the maximum degradation rate and the char residue at 600°C of Cast PHBV and C-PHBV/3C30B bionanocomposite as a function of irradiation dose

Samples	Dose (kGy)	$T_{5\%}$ (°C)	$T_{50\%}$ (°C)	Tmax. rate T_{vmd} (°C)	Char (%) at 600(°C)
PHBV	0	263 ± 1	282 ±1	285 ± 0.5	1.3 ± 0.1
	5	258 ± 0.5	278 ± 0.5	282 ± 0.5	1.5 ± 0.2
	25	260 ± 0.5	279 ± 0.00	283 ± 1	1.6 ± 0.1
	100	258 ± 0.5	278 ± 0.5	282 ± 1	1.5 ± 0.1
PHBV/3C30B	0	266 ± 1	290 ± 1	293 ± 1	3.6 ± 0.2
	5	266 ± 1	288 ± 0.5	293 ± 0.5	4.2 ± 0.2
	25	264 ± 1	284 ± 1	289 ± 0.0	4.5 ± 0.1
	100	259 ± 0.5	285 ± 0.5	288 ± 1	4.0 ± 0.1

3.5 Changes in Thermo-Mechanical Behaviour

Figs. 3(a), 3(b) represent the curves of storage modulus (G') for Cast PHBV and C-PHBV/3C30B bionanocomposite before and after gamma irradiation at various doses from 0 to 100 kGy. The results indicate an enhancement of storage modulus (G') for the bionanocomposite compared to that of Cast PHBV before gamma irradiation. This may be related to the favorable interactions and large interfacial area developed between the polymer matrix and C30B organoclay that should restrict the movement of polymer chains [16,29].

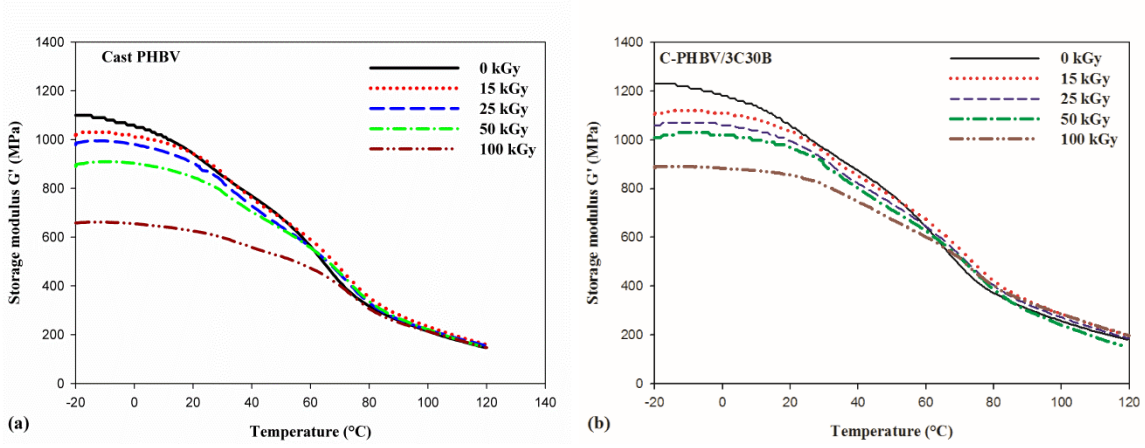

Figure 3: Temperature dependence of storage modulus (G') for (a): Cast PHBV and (b): C-PHBV/3C30B bionanocomposite at various doses

After gamma irradiation, it is observed that the storage modulus blow the α-transition of both Cast PHBV and C-PHBV/3C30B bionanocomposite, which is reduced with increasing irradiation dose (Figs. 3(a), 3(b). In our previous study the same trend was observed for the Cast PHBV and C-PHBV/3C30B nanobiocomposites exposed to UV irradiation [30]. This phenomenon could be due to the significant reduction in both molecular weights and crystallinity index related to the radiation degradation of PHBV

via chain scission mechanisms [21,30]. We can also notice that C-PHBV/3C30B bionanocomposite was less affected by gamma irradiation; a lower decrease in storage modulus compared to Cast PHBV is observed, e.g., at -20°C after irradiation at 100 kGy, G' is decreased of 35.1% and 27.2% for Cast PHBV and the bionanocomposite, respectively. The incorporation of C30B in PHBV matrix thus allows counterbalancing the radiolytic degradation of PHBV chains by better maintaining the thermo-mechanical properties of the material between -20 to 60°C. Above this temperature range, gamma irradiation and the presence of C30B have nearly no effect, G' being similar (roughly 200 MPa) for all the materials (i.e., irradiated or not and with or without C30B).

3.6 Tensile Properties Changes

The changes in the mechanical properties after gamma irradiation of Cast PHBV and C-PHBV/3C30B bionanocomposite were investigated using tensile tests. Figs. 4(a), 4(b) and Figs. 5(a), 5(b), 5(c) show the tensile curves, the evolution of Young's modulus, tensile strength and elongation at break of Cast PHBV and C-PHBV/3C30B bionanocomposite samples as function of irradiation dose from 0 to 100 kGy. Regarding the tensile behaviour, the mechanical response of irradiated samples strongly depend on the irradiation dose, the material being less stiff and more brittle with increasing irradiation dose. Indeed, tensile strength of Cast PHBV decreased from 31.6 ± 1.1 to 28.3 ± 0.9, 27.1 ± 1.2 and 14.1 ± 2.8 for specimens irradiated at 15, 25 and 50 kGy respectively. At 100 kGy, the irradiated PHBV becomes extremely brittle with a significant decrease in both tensile strength and elongation at break value from 31.6 to 1.4 MPa and from 0.80% to 0.13%, respectively. This phenomenon is explained as a result of the degradation of PHBV matrix and drastic reduction of molecular weight. Similar trend were reported by Hermida et al. [8] for irradiated PHB and PHBV at 10, 20, 40, 80 and 180 kGy.

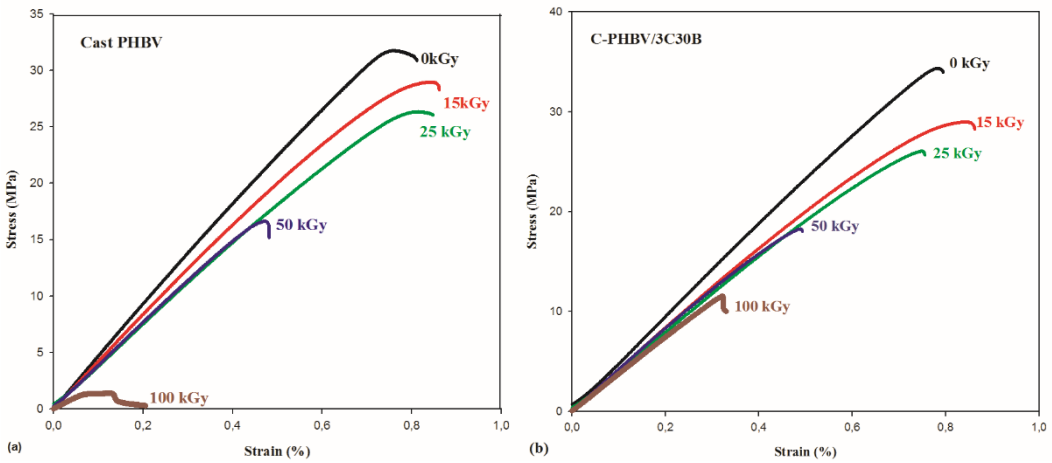

Figure 4: Curves of tensile stress versus strain for (a): Cast PHBV and (b): C-PHBV/3C30B bionanocomposite at various doses

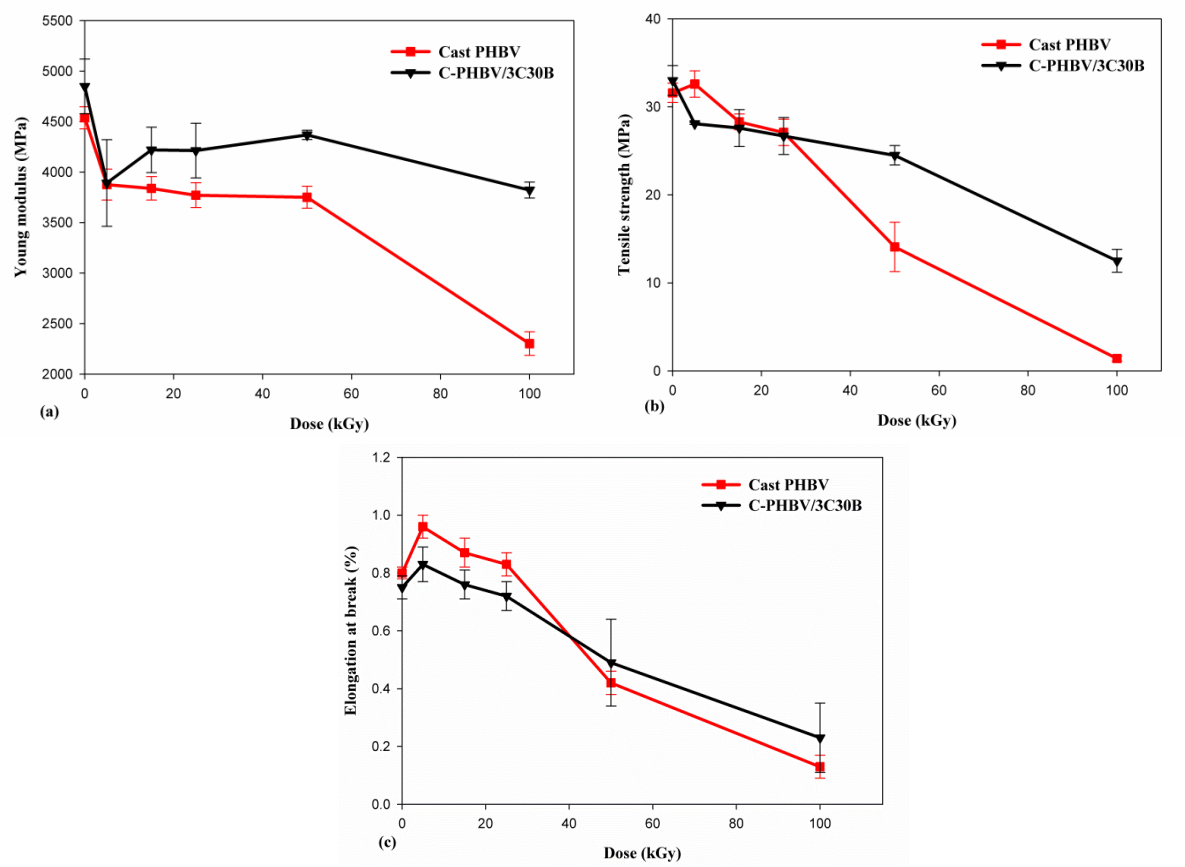

Figure 5: Evolution of (a) Young's modulus, (b) tensile strength,(c) elongation at break for Cast PHBV and C-PHBV/3C30B as a function of irradiation dose

As observed on Fig. 4(b), the irradiated bionanocomposites samples were less brittle compared to the Cast PHBV, and lower loss in the elastic and ultimate tensile properties was obtained. For C-PHBV/3C30B the tensile strength decreases from 33 ± 1.7 MPa to 27.6 ± 2.1, 26.7 ± 2.1, 24.5 ± 1.1 and 12.5 ± 1.3 MPa for specimens irradiated at 15, 25, 50 and 100 kGy respectively. In contrast with literature [5,8], the tensile modulus of Cast PHBV decreases significantly with increasing the irradiation dose by about 15.4, 16.9, 17.3 and 49.3% for doses at 15, 25, 50 and 100 kGy respectively. The decrease of tensile modulus of Cast PHBV with increasing the dose may be attributed to the decrease in the molecular weight resulting in the formation of polymer chains of smaller length. Another explanation is that this phenomenon could also be a consequence of the decrease of crystallinity in the irradiated PHBV matrix [19,26,31]. The irradiated C-PHBV/3C30B bionanocomposite shows a more limited decrease in tensile modulus compared to Cast PHBV. Indeed, the Young's modulus was reduced by 9.7, 9.7, 10.0 and 21.1% at doses of 15, 25, 50 and 100 kGy, respectively. This can be explained by improvement of the clay dispersion after gamma irradiation as shown by TEM observations in Fig. 8. As observed for the thermo-mechanical analysis, the incorporation of C30B clays appears to counterbalance the radiolytic degradation of PHBV chains by better maintaining the tensile properties of the material.

3.7 Morphologies Changes

Figs. 6(a) and 6(b) shows SEM micrographs of the fractured surface of the Cast PHBV before and after gamma irradiation at 100 kGy at a magnification of 2000. Before exposure, as shown in Fig. 6(a), the fractured surface of the Cast PHBV sample exhibits an irregular fractured surface due to its crystalline structure.

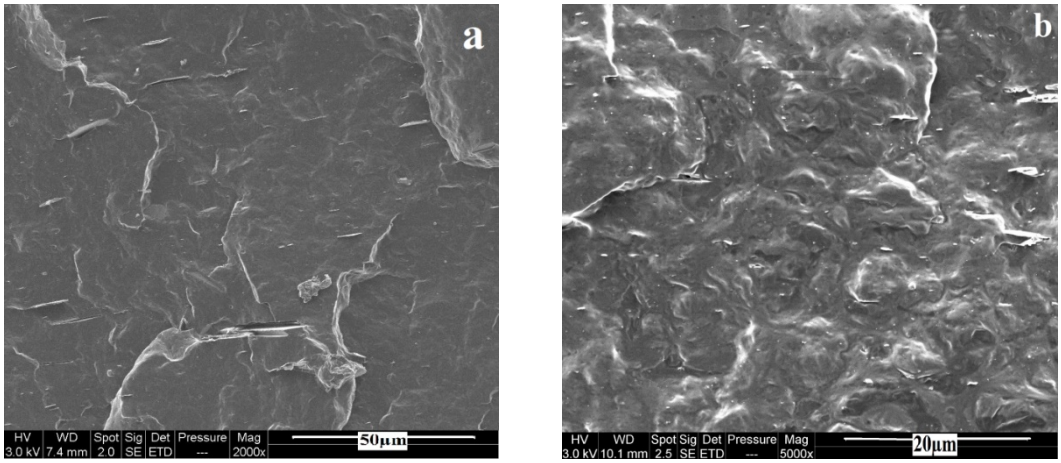

Figure 6: SEM micrographs (× 2000) of fractured surface (a) Cast PHBV before irradiation (b): Cast PHBV after irradiation at 100 kGy

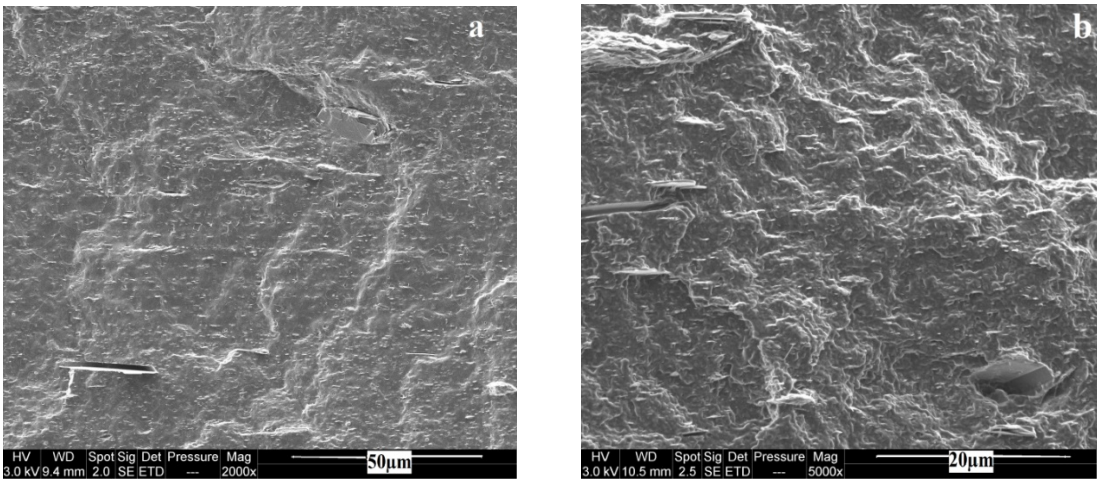

Figure 7: SEM micrographs (× 2000) of fractured surface, (a): C-PHBV/3C30B before irradiation (b): C-PHBV/3C30B after irradiation at 100 kGy

After gamma irradiation at 100 kGy, the fractured surface (Fig. 6(b)) of the sample is characterized by a rough surface, the appearance of voids, some irregularities and defects, due to degradation of the material. However, the damage is much less pronounced for the PHBV bionanocomposite samples, which are characterized by lower degradation rate. Indeed, the morphological changes due to gamma irradiation in the C-PHBV/3C30B bionanocomposite are shown in Figs. 7(a) and 7(b) and the fractured surface of C-PHBV/3C30B bionanocomposite exhibits a slightly rough surface before exposure. The appearance of voids or defects was not observed in this case and irradiated C-PHBV/3C30B films do not present noticeable damages. To investigate the effects of gamma irradiation on both orientation and dispersion state of C30B within the PHBV matrix, TEM analysis was conducted. Indeed, Fig. 8(a) shows the TEM micrograph of the non-irradiated C-PHBV/3C30B bionanocomposite, and Figs. 8(b) and 8(c) those

irradiated at 50 and 100 kGy, respectively. The micrograph in Fig. 8(a) indicates the presence of some dispersed platelets of organoclays, suggesting an intercalated structure. However, at radiation dose of 50 and 100 kGy, the TEM observations display the presence of some individual layers in the PHBV matrix besides some layer stacks as shown in Figs. 8(b) and 8(c), respectively. Indeed, this suggests the formation of a partially exfoliated structure in the bionanocomposite at higher doses. This phenomenon, reported by Zaidi et al. [9] has been attributed to better interactions between the clay layers and the oxygenated species formed during the radiolytic degradation of PHBV, leading to better dispersion of the C30B in the polymer matrix.

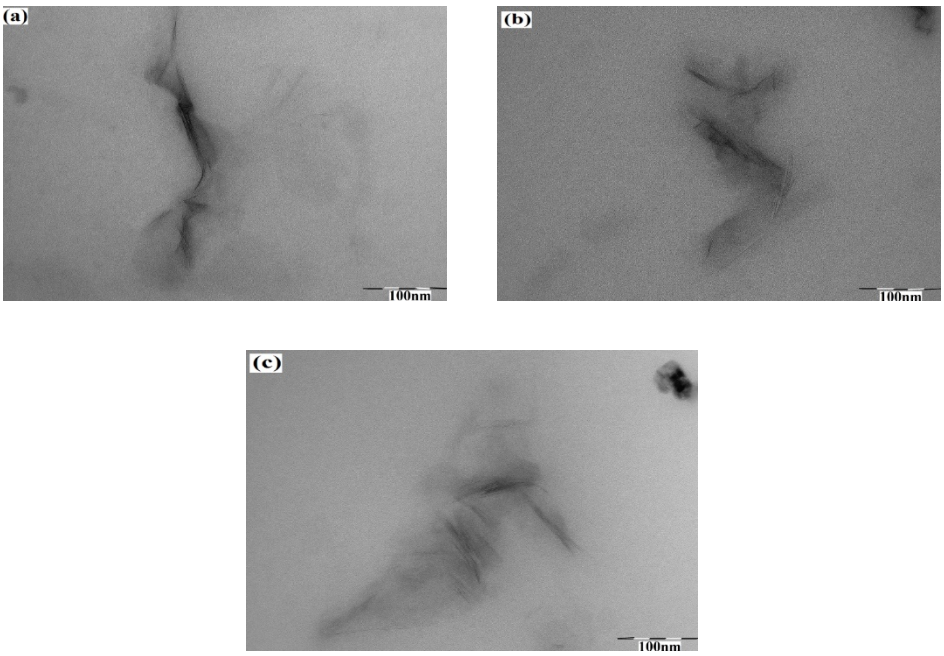

Figure 8: TEM micrographs of C-PHBV/3C30B bionanocomposite (a): Before irradiation, (b): After irradiation at 50 kGy and (c): After gamma irradiation at 100 kGy

4 Conclusion

From the study, it can be concluded that gamma irradiation of Cast PHBV and PHBV/C30B bionanocomposite investigated in the dose range 5-100 kGy, results in the decrease in $\overline{M_w}$, $\overline{M_n}$ and Đ with increasing the dose, suggesting the occurrence of random chain scission, which is however more pronounced for the neat polymer. Gamma irradiation also affects the thermal properties of irradiated samples. Indeed, the DSC thermograms of both Cast PHBV and C-PHBV/3C30B exhibit double melting peaks above 15 kGy, while crystallinity index (Xc) and melting temperature decrease with increasing the dose. Both Cast PHBV and PHBV/3C30B exhibit almost similar thermal stability under gamma irradiation exposure characterized by a very small decrease in the $T_{5\%}$ value at 100 kGy compared to the reference samples. Mechanical results indicate a decrease in tensile modulus, tensile strength and elongation at break of C-PHBV/3C30B bionanocomposite and Cast PHBV with increasing the radiation dose; being however less pronounced for the bionanocomposite. Storage modulus (G') also decreases with increasing the dose for both Cast PHBV and PHBV/3C30B bionanocomposite samples. All results lead to the conclusion that the incorporation of Cloisite 30B to PHBV allows counterbalancing the detrimental effect of radiochemical degradation on the properties of irradiated PHBV.

Acknowledgments: I.K. gratefully acknowledges the Averroes program for financial support (Averroes 4), in the framework of the Erasmus Mundus European program.

References

1. Bugnicourt, E., Cinelli, P., Lazzeri, A., Alvarez, V. (2014). Polyhydroxyalkanoate (PHA): review of synthesis, characteristics, processing and potential applications in packaging. *Express Polymer Letters, 8(11),* 791-808.
2. Santos, R. F. S., Araujo, E. S., Ferreira, C. R. C., Ribeiro, A. S. (2009). Radiolytic stabilization of poly(hydroxybutyrate). *Radiation Physics and Chemistry, 78,* 85-91.
3. Ahmadi, S. J., Huang, Y. D., Ren, N., Mohaddespour, A., Ahmadi-Brooghani, S. Y. (2009). The comparison of EPDM/clay nanocomposites and conventional composites in exposure of gamma irradiation. *Composites Science and Technology, 69,* 997-1003.
4. Yildirim, Y., Oral, A. (2014). The influence of γ-ray irradiation on the thermal stability and molecular weight of Poly(L-Lactic acid) and its nanocomposites. *Radiation Physics and Chemistry, 96,* 69-74.
5. Luo, S., Netravali, A. N. (1999). Effect of ^{60}Co γ-radiation on the properties of poly(hydroxybutyrate-co-hydroxyvalerate). *Journal of Applied Polymer Science, 73,* 1059-1067.
6. Mitomo, H., Watanabe, Y., Ishigaki, I., Saito, T. (1994). Radiation-induced degradation of poly(3-hydroxybutyrate) and the copolymer poly(3-hydroxybutyrate-co-hydroxyvalerate). *Polymer Degradation and Stability, 45,* 11-17.
7. Oliveira, L. Araujo, M. E. S., Guedes, S. M. L. (2006). Gamma irradiation effects on poly(hydroxybutyrate). *Polymer Degradation and Stability, 91,* 2157-2162.
8. Hermida, E. B., Mega, V. I., Yashchuk, O., Fernandez, V., Eisenberg, P. et al. (2008). Gamma irradiation effects on mechanical and thermal properties and biodegradation of poly(3-hydroxybutyrate) based films. *Macromolecular Symposia, 263,* 102-113.
9. Zaidi, L., Bruzaud, S., Kaci, M., Bourmaud, A., Gautier, N. et al. (2013). The effects of gamma irradiation on the morphology and properties of polylactide/Cloisite 30B nanocomposites. *Polymer Degradation and Stability, 98,* 348-355.
10. Zembouai, I., Kaci, M., Bruzaud, S., Dumazert, L., Bourmaud, A. et al. (2016). Gamma irradiation effects on morphology and properties of PHBV/PLA blends in presence of compatibilizer and Cloisite 30B. *Polymer Testing, 49,* 29-37.
11. Zembouai, I., Kaci, M., Bruzaud, S., Pillin, I., Audic, J. L. et al. (2016). Electron beam radiation effects on properties and ecotoxicity of PHBV/PLA blends in presence of organo-modified montmorillonite. *Polymer Degradation and Stability, 132,* 117-126.
12. Marra, A., Boumail, A., Cimmino, S., Criado, P., Silvestre, C. et al. (2016). Effect of PLA/ZnO packaging and gamma radiation onthe content of *listeria innocua, escherichia coli* and *salmonella enterica* on ham during storage at 4°C. *Journal of Food Science and Engineering, 6,* 245-259.
13. Mizera, A., Stoklasek, P., Bednarik, M. (2017). Physical properties of polyamide 11 after radiation cross-linking by accelerated electrons. *Key Engineering Materials, 756,* 19-26.
14. Aouat, T., Kaci, M., Lopez-Cuesta, J. M., Devaux, E., Mahlous, M. (2018). The effect of gamma-irradiation on morphology and properties of melt-spun poly (lactic acid)/cellulose fibers. *Polymer Degradation and Stability.* https://doi.org/10.1016/j.polymdegradstab.2018.11.014.
15. Cassan, D., Hoheisel, A. L., Glasmacher, B., Menzel H. (2019). Impact of sterilization by electron beam, gamma radiation and Xrays on electrospun poly-(ε-caprolactone) fiber mats. *Journal of Materials Science: Materials in Medicine, 30,* 42.
16. Iggui, K., Le Moigne, N., Cambe, S., Degorce-Dumas, J. R., Kaci, M. et al. (2015). A biodegradation study of poly(3-hydroxybutyrate-co-3-hydroxyvalerate)/organoclay nanocomposites in various environmental conditions, *Polymer Degradation and Stability, 119,* 77-86.
17. Rosario, F., Corradini, E., Casarin, S. A., Agnelli, J. A. M. (2013). Effect of gamma radiation on the properties of poly(3-hydroxybutyrate-co-hydroxyvalerat)/poly(ε-caprolactone) blends. *Journal Polymer Environment, 21,* 789-794.
18. Barham, P. J., Keller, A., Otun, E. L., Holmes, P. A. (1984). Crystallization and morphology of a bacterial thermoplastic: Poly-3-hydroxybutyrate. *Journal Materials Science, 19,* 2781-2794.

19. Bergmann, A., Tebmar, J., Owen, A. (2007). Influence of electron irradiation on the cryslallisation, molecular weight and mechanical properties of poly-(R)-3-hydroxybutyrate. *Journal Materials Science, 42,* 3732-3738.
20. Miyazaki, S. S., Yep, A. R., Kolton, F., Hermida, E. B., Povolo, F. (2003). Biodegradable polymeric films based on microbial poly(3-Hydroxybuterate). Effect of gamma-radiation on mechanical properties and biodegradability. *Macromolecular Symposia, 197,* 57-64.
21. Parra, D. F., Rosa, D. S., Rezende, J., Ponce, P., Lugao, A. B. (2014). Biodegradation of γ irradiation poly 3-hydroxybutyrate (PHB) films blended with poly(ethyleneglycol). *Journal Polymer Environment, 19,* 918-925.
22. Parra, D. F., Rodrigues, J. A. F. R., Lugao, A. B. (2005). Use of gamma irradiation technology in the manufacture of biopolymer-based packaging films for shelf-stable foods. *Nuclear Instruments and Methods in Physics Research B, 236,* 563-566.
23. Abrishami, S. A., Chakoli, A. N. (2019). Effect of radiation processing on physical properties of aminated MWCNTs/Poly(L-lactide) nanocomposites. *Composites Communications, 14,* 43-47.
24. Shahabi-Ghahfarrokhi, I., Khodaiyanb, F., Mousavi, M., Yousefic, H. (2015). Effect of γ-irradiation on the physical and mechanical properties of kefiran biopolymer film. *International Journal of Biological Macromolecules, 74,* 343-350.
25. Touati, N., Kaci, M., Ahouari, H., Bruzaud, S., Grohens, Y. (2007). The Effect of γ-Irradiation on the structure and properties of poly(propylene)/clay nanocomposites. *Macromolecular Materials Engineering, 292,* 1271-1279.
26. Zaidi, L., Bruzaud, S., Bourmaud, A., Médéric, P., Kaci, M. et al. (2010). Relationshipbetween structure and rheological, mechanical and thermal properties of polylactide/Cloisite 30B nanocomposites. *Journal of Applied. Polymer Science, 116,* 1357-1365.
27. Zaidi, L., Kaci, M., Bruzaud, S., Bourmaud, A., Grohens, Y. (2010). Effect of natural weather on the structure and properties of polylactide/Cloisite 30B nanocomposites. *Polymer Degradation and Stability, 95,* 1751-1758.
28. Chen, G. X., Hao, G. J., Guo, T. Y., Song, M. D., Zhang, B. H. (2002). Structure and mechanical properties of poly(3-hydroxybutyrate-co-3-hydroxyvalerate) (PHBV)/clay nanocomposites. *Journal Materials Science, 21,* 1587-1589.
29. Iggui, K., Kaci, M., Le Moigne, N., Bergeret, A. (2018). The effects of accelerated photooxidation on molecular weight and thermal and mechanical properties of PHBV/Cloisite 30B bionanocomposites. *Journal of Renewable Materials, 6(11),* 288-298.
30. Chikh, A., Benhamida, A., Kaci, M., Bourmaud, A., Bruzaud S. (2017). Recyclability assessment of poly(3-hydroxybutyrate-co-3-hydroxyvalerate)/poly(butylene succinate) blends: combined influence of sepiolite and compatibilizer. *Polymer Degradation and Stability, 142,* 234-243.